



ELSEVIER

Contents lists available at ScienceDirect

Journal of Petroleum Science and Engineering

journal homepage: www.elsevier.com/locate/petrol

Preliminary evaluation of gas content of the No. 2 coal seam in the Yanchuannan area, southeast Ordos basin, China



Yidong Cai^a, Dameng Liu^{a,*}, Keming Zhang^a, Derek Elsworth^b, Yanbin Yao^a, Dazhen Tang^a

^a Coal Reservoir Laboratory of National Engineering Research Center of CBM Development & Utilization, China University of Geosciences, Beijing 100083, China

^b G3 Center, EMS Energy Institute, and Department of Energy and Mineral Engineering, Pennsylvania State University, University Park, PA 16801, USA

ARTICLE INFO

Article history:

Received 12 December 2013

Accepted 16 September 2014

Available online 28 September 2014

Keywords:

gas content

geological controls

Yanchuannan area

SE Ordos Basin

ABSTRACT

Gas contents are highly variable in coalbed methane (CBM) reservoirs of the Yanchuannan (YCN) area of the southeast (SE) Ordos Basin, China. We used diverse geologic data derived from more than five years of exploration to provide insight into the origin of this variability and the consequences of gas content on reservoir performance. Major factors affecting gas content variability include gas generation, migration, trapping and preservation. Gas generation affects gas content variability on the scale of the total resource, whereas gas migration influences the inhomogeneous redistribution of gas content on a regional or local scale. Gas trapping and preservation affect the “as-observed” content. The potential for high gas content is controlled directly by the composite result of gas generation, migration, trapping and preservation. CBM in the YCN area is produced from the relatively thick seam (~2.09 m and 8.05 m, with an average of 5.97 m) that is distributed through 450–1200 m of the stratigraphic section. Gas content tends to be structurally and hydrodynamically controlled in the order of simple structure (folds and small faults) > complex structure (large regional faults) and groundwater stagnant zones > runoff zones. Coal samples in the YCN area typically have Langmuir volumes between 31.86 and 46.51 cm³/g, which correlates with coal rank. Reservoir heterogeneity including coal composition, pore structure and matrix moisture content may contribute to the heterogeneous gas content. Gas content is generally high where hydrodynamic trapping of gases occurs and may be anomalously low in areas of active recharge with downward flow potential and/or convergent flow where there is no mechanism for entrapment. In the YCN area, the most favorable area for CBM exploration and development is in the center block (block B), where great coal thickness, moderate burial depth, favorable hydrodynamics and an anticlinal trap coincide to yield high gas contents.

© 2014 Elsevier B.V. All rights reserved.

1. Introduction

CBM recovery from coal seams will both benefit mining safety and reduce greenhouse gas emission (Karacan et al., 2011). In addition, with the decline in conventional natural gas reserves and increased demand and price of gas, industry shows great interest in unconventional gas (CBM, shale gas) resources, which requires accurate estimation of CBM/shale gas potential and recoverable reserves to assist in its development. CBM resources are abundant in the middle-high rank coals distributed throughout the targeted southern Qinshui Basin (Su et al., 2005; Cai et al., 2011; Song et al., 2012; Liu et al., 2014) and the eastern Ordos Basin (Xu et al., 2012), China. Although many CBM exploration and basic research projects have been initiated, only a few studies on

the preliminary regional CBM reservoir and resources have been conducted in the eastern Ordos Basin. This area has become a focus of much research and offers a new field of CBM exploration and development (Zhang et al., 2010; Tao et al., 2012; Xu et al., 2012).

The Ordos Basin is the second fastest developing district of the CBM industry in China. Large and diverse databases have been assembled on the geology and performance of CBM reservoirs in the Ordos Basin (Yao et al., 2009; Wei et al., 2010; Zhang et al., 2010; Tang et al., 2012; Yao et al., 2013) and on the assessment of CBM potential (Feng et al., 2002; Jie, 2010; Lu et al., 2011). The SE Ordos Basin has medium to high rank coals that have the great potential for CBM development. Previous studies estimated that the gas in place (GIP) for CBM in place in the eastern Ordos Basin and the entire Ordos Basin are about 9×10^{12} m³ (Jie, 2010) and 10.72×10^{12} m³ (Feng et al., 2002), respectively.

The YCN area covers an area of 679.6 km², which is considered to be the second CBM commercial pilot after the Southern Qinshui

* Corresponding author. Tel.: +86 10 82320892 (office); fax: +86 10 82326850.

E-mail address: dmliu@cugb.edu.cn (D. Liu).

basin. Until March of 2012, 45 test and production wells were drilled in the YCN area, which has become the first CBM pilot-production field of Sinopec. Thirty-three wells have each produced about 16,000 m³ of gas per day, accounting for a cumulative gas production of 284.6×10^4 m³. In addition, 10 of these wells have gas production over 1000 m³/d. Based on well testing results, the initial reservoir pressure ranges from 3.6 MPa to 10 MPa. Desorption pressure ranges from 2.19 MPa to 9.88 MPa, with an average of 3.58 MPa, which is favorable for gas desorption. The highest CBM production is ~ 2632 m³ per day. CBM proved reserves of the YCN area have remained relatively constant but have increased slightly over the past four years with increased CBM exploration and development for more deeply buried deposits. Because of this significant gas potential, the YCN area is considered favorable for CBM exploration and development. The increase in proved CBM reserves, despite the significant increase in production, is attributed to the efforts of smaller operators and independents in finding new reserves. CBM production and reserves are expected to increase as exploration continues in unexplored areas and as secondary recovery techniques using N₂, CO₂, or biotechnologies are employed (Busch and Gensterblum, 2011; Connell et al., 2011; Fallgren et al., 2013).

Understanding the factors that controlled gas content in coals is critical to developing an effective and successful exploration program. Therefore, we review the key geologic factors that affect gas content and discuss how these factors ultimately determine the gas content in coals. An evolution model of gas content based on a decade of CBM research in China is proposed (Fig. 1), which can be used to predict areas of unusually high gas content and, of equal importance areas of unusually low gas content values.

Large and diverse databases have been assembled on the geology and reservoir performance of the No. 2 coal seam in the SE Ordos Basin (Feng et al., 2002; Yao et al., 2009; Wei et al., 2010; Zhang et al., 2010; Jie, 2010; Lu et al., 2011; Tang et al., 2012). This paper synthesizes the available geologic, hydrologic, petrologic, and reservoir information to provide perspective on the ways that variable factors influence the gas content and therefore the viability of the CBM field for production. We begin with a review of the geologic framework of the SE Ordos CBM fields and continue

with an evolution model of gas content. We, then follow with a discussion of factors controlling gas content. Finally, the paper concludes with a discussion of the relationship of gas content with related geologic variables.

2. Geologic framework

During the Cambrian to Ordovician periods, shallow marine carbonate was deposited on the ancient crystalline basement in the Ordos Basin following stable crustal subsidence (Stauffer et al., 2009). The Ordos Basin is located in northern China, which covers about 320,000 km². Thickness of sedimentary fill of the basin approach 5000 m. The Ordos Basin has been through three orogenies; the Indosinian, Yanshanian and Himalayanian orogenies. The deposited coal-bearing strata of the Carboniferous and Permian were altered by these three orogenies (Fig. 2).

The Ordos Basin can be subdivided into six structural units, including the Yimeng Uplift, the Weibei Uplift, the Jinxi Fault-fold Belt, the Yishan Slope, the Tianhuan Depression, and the Western Edge Fault Belt (Liao et al., 2007). The YCN area is located in the Hedong fault-fold belt (Zhang et al., 2011; Lu et al., 2011), which is within the Jinxi fault-fold belt (Lu et al., 2011), and near the SE edge of the Ordos Basin. Folds within the YCN area are not well developed. Only two folds exist in the northeast YCN area with 10–17 km NE axial strike. Strata of these two anticlinal wings are normally flat with a dip angle of $\sim 8^\circ$. The axial strike of most of the faults in the YCN area is NNE, NE and near S–N, partially E–W, which is consistent with the regional tectonics. The central YCN area is developed in two large NE-trending thrust faults (Fig. 3). In the southeastern edge of the YCN area, there is a normal fault.

3. Evolution model of gas content

Gas content, one of the most important controls on CBM producibility, is one of the most difficult parameters to accurately assess. Gas content is not fixed, but changes when equilibrium conditions within the reservoir are disrupted and is strongly dependent upon multiple geologic factors and reservoir conditions (Scott et al., 1994; Scott and Kaiser, 1996). The distribution of gas content varies laterally within individual thin coal seams, vertically among coals within a single well, and laterally and vertically within thick coal seams.

In general, gas content increases with depth and coal rank, but is often highly variable due to geological heterogeneities, coal composition and/or vagaries related to the analytical laboratory. Previous research has indicated that initial pressure increases gas content but that this effect diminishes ~ 1000 m (Gensterblum et al., 2014). Although determination of migration direction for gas generally implies conventional gas, gas content in coals can be rebalanced, either locally, regionally or vertically, by generation of secondary biogenic gases or by diffusion and long-distance migration of thermogenic and secondary biogenic gases to no-flow structural boundaries such as hingelines or faults for eventual resorption and conventional trapping (Scott, 2002). Therefore, migration direction through isotopic and hydrodynamic studies is critical for determining the areas of higher gas content. Finally, good preservation conditions of CBM reservoirs are the last step for high CBM producibility. Therefore, gas content is a composite result of multiple factors including geologic, hydrodynamic, and petrophysical conditions and reservoir characteristics.

Exceptionally high gas contents do not necessarily guarantee high production rates if permeability is too low (Scott and Kaiser, 1996). And low sealing capability of roof lithology and thickness may also cause low gas content. Assuming that gas content reported from field test are reasonably accurate, there are many

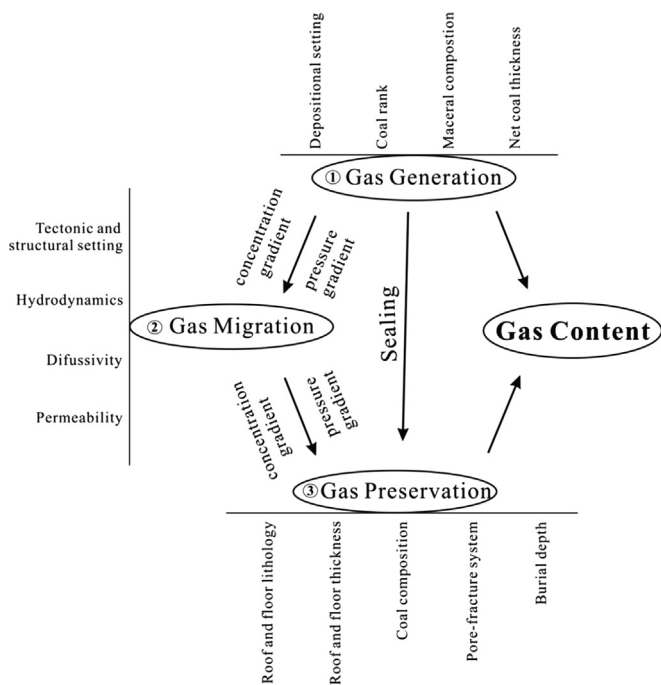


Fig. 1. An evaluation model of gas content.

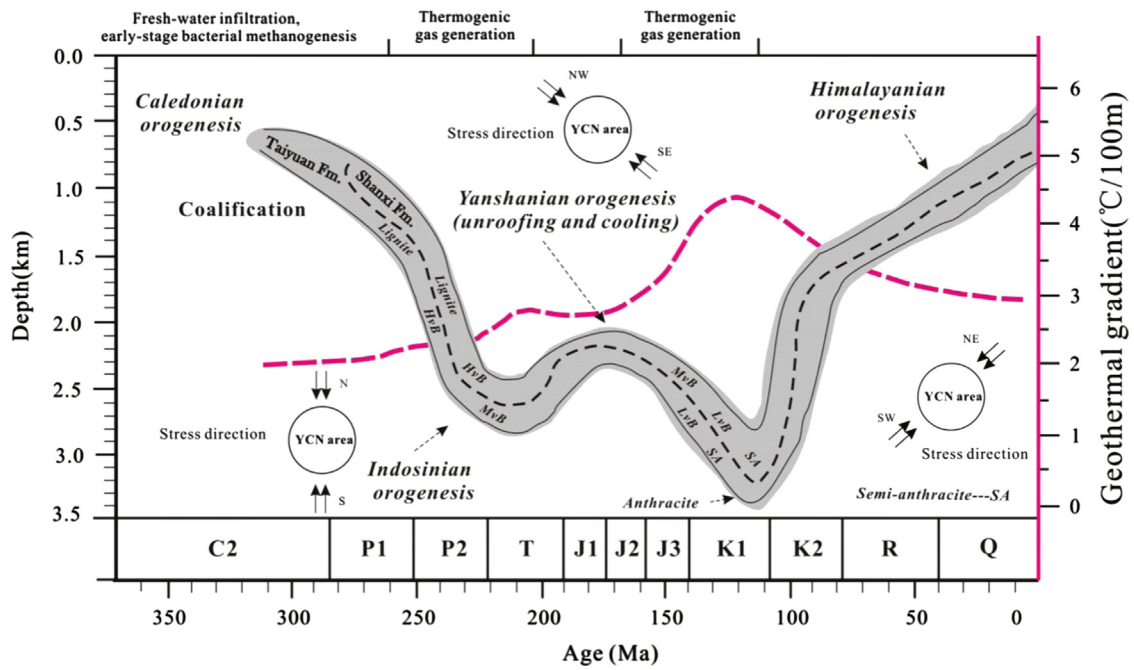


Fig. 2. Generalized tectonic movement, temperature and burial history curve for coal-bearing strata in the YCN area, SE Ordos Basin (data of pink line from Ren et al., 2006).

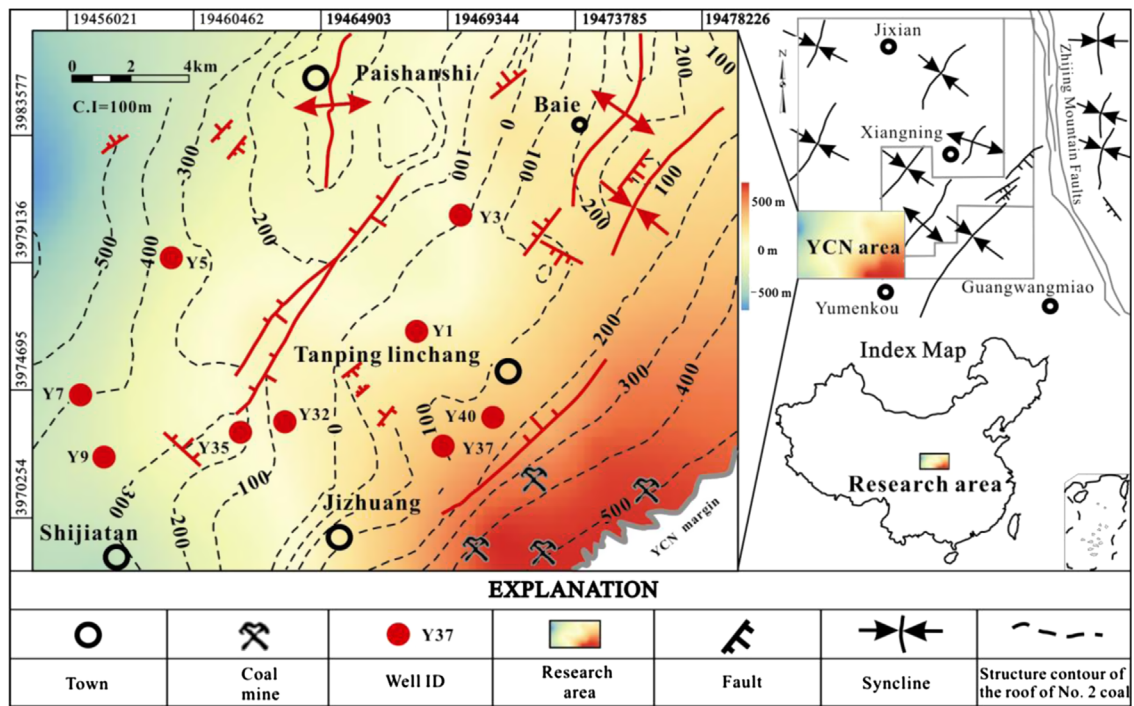


Fig. 3. Structure top of the No. 2 coal seam in the YCN area of the SE Ordos Basin.

geologic and reservoir factors that affect the distribution of CBM in the subsurface. These factors can be divided into four categories, which are (1) gas generation, (2) migration, (3) trapping and (4) preservation (Fig. 1). These factors will be discussed in greater detail below. Data used in this paper include coal thickness, maximum vitrinite reflectance ($R_{o,m}$), burial depth, roof/floor lithology, in-place gas content and hydrodynamics. Data were collected from 40 exploration wells and partly from analyses of nine coal samples (including microfractures, coal compositions, petrophysical characteristics), which were documented as previously (Cai et al., 2011).

4. Factors affecting gas content

4.1. Gas generation

4.1.1. Depositional setting

Coal seams are dispersed though a thick stratigraphic section dominated by paralic clastic strata. The principal coal seams targeted for CBM exploration in the YCN region are within the Taiyuan Formation of the Upper Pennsylvanian No. 10 coal and the Shanxi Formation of the Lower Permian No. 2 coal (Fig. 4). Coals in the Shanxi and Taiyuan Formations are commonly bright-banded

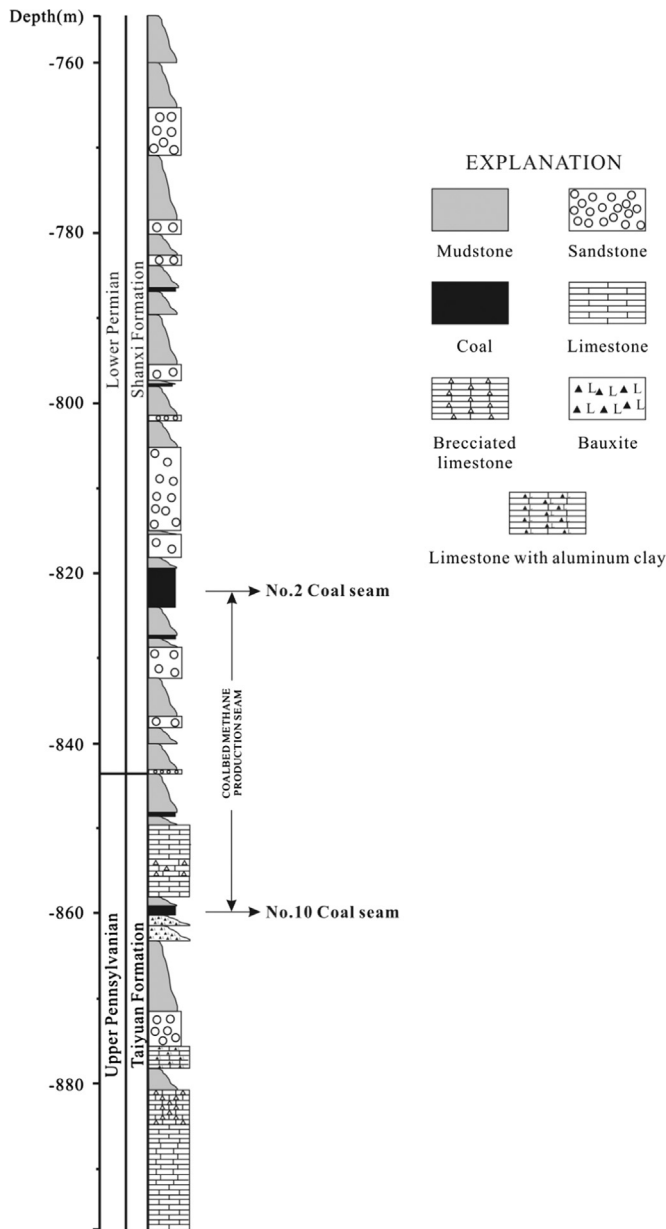


Fig. 4. Stratigraphic section of the YCN area in the SE Ordos Basin.

and are of bituminous–anthracite rank. The thickness of individual seams ranges from less than 0.8 m to more than 8.0 m, and seams as thick as 2 m are commonly targeted for production. Two main coal seams have been intersected in all vertical wells, although more than 3 seams have been found in some wells in the YCN area.

The Lower Permian strata are of deltaic plain origin and exhibit a stable paralic depositional cyclicity. Coal depositional trends orthogonal to gas migration pathways will potentially allow migrating gas to be trapped at permeability barriers associated with facies changes (Scott, 2002). Normally, the effects of depositional environment on CBM generation include: (1) coal thickness and structure; and (2) coal quality. Coal from ligneous plants can produce more gas than that of herbaceous plant during coalification. The deltaic plain environment of this particular study would have provided suitable moisture and temperature for ligneous plants as the basis for the generated gases. The upper Taiyuan Formation is composed of gray mudstone, siltstone, sandstone and thick coal of tidal flat origin and show facets of marine deposition. The lower Permian Shanxi Formation is composed of gray mudstone,

muddy siltstone, carbonaceous mudstone, bauxite, brecciated limestone, limestone with aluminum clay, limestone, and thickly bedded coal (Fig. 4). The Shanxi Formation is of fluvial-deltaic origin and exhibits a strong transgressive-regressive depositional cyclicity, which has been interpreted as a product of high-frequency eustatic sea-level changes (Pashin, 2010). A result of this cyclicity is that coals are clustered in a series of coastal plain. Overall, the No. 2 and No. 10 coal seams are stably distributed in the YCN area. The No. 2 coal seam is 2–8 m thick, with an average of 6 m (Table 1), and the No. 10 coal seam varies in thickness from 0.8 to 6.5 m, with an average of 2.6 m. Gas content of the No. 2 coal seam ranges from 0.2 to 20.3 m³/t with an average of 9.2 m³/t. Totally, the coal thickness decreases from southeast (~8 m) to northwest (~3 m) (Fig. 5). And several thick coal accumulations occur in the center of the YCN area, which should have been controlled by the late Triassic squeezing tectonic movement.

4.1.2. Coal composition and coal ranks

Coals from the SE edge of the YCN area are composed of 47–96% vitrinite, 4–49% inertinite, 0–10% liptinite (Table 2) and some other accessory minerals including pyrite. High vitrinite content of the YCN coals shows that this area was in a closed sedimentary environment, which is conducive to CBM generation. From the available data, the porosity and permeability of coals in the YCN is low (normally < 0.2 mD) (Table 3), which should affect CBM

Table 1

R_o , m , coal thickness, depth, roof lithology and G_i of the No. 2 coal seam in the YCN area.

Well name	R_o , m (%)	Coal rank	Coal thickness (m)	Depth (m)	Roof lithology	G_i (m ³ /t)
Y 1	1.98	lvb	5.47	855	Mudstone	9.92
Y 2	1.95	lvb	5.81	804	Mudstone	x
Y 3	1.92	lvb	5.5	903.9	Mudstone	7.43
Y 4	x	lvb*	5.58	850.6	Mudstone	5.36
Y 5	2.11	sa	4.56	1103.5	Mudstone	1.18
Y 6	1.95	lvb	6	770.5	Mudstone	8.73
Y 7	2.05	sa	4.5	1030.6	Mudstone	20.38
Y 8	1.91	lvb	5.78	805.8	Mudstone	x
Y 9	2.01	sa	3.55	824.64	Mudstone	x
Y 10	x	lvb*	5.63	855.9	Mudstone	x
Y 11	2	sa	4.59	1080.7	Mudstone	x
Y 12	1.87	lvb	5.79	725.75	Mudstone	x
Y 13	1.97	lvb	5.49	1043.6	Mudstone	x
Y 14	2.08	sa	5.63	907.6	Siltstone	8.06
Y 15	1.97	lvb	4.81	911.3	Mudstone	x
Y 16	2	sa	5.8	825.46	Mudstone	14.24
Y 17	1.64	lvb	5.65	572.48	Siltstone	2.35
Y 18	2.2	sa	5.37	934.8	Mudstone	x
Y 19	1.98	lvb	4.94	945.34	Mudstone	x
Y 20	1.94	lvb	6.46	828.45	Mudstone	6.11
Y 21	2.01	sa	5.15	848.5	Mudstone	x
Y 22	x	lvb*	5.57	753.4	Mudstone	x
Y 23	1.46	m vb	5.03	541.45	Siltstone	0.2
Y 24	1.48	m vb	4.3	463.89	Mudstone	1.28
Y 25	x	lvb*	5.46	780.4	Mudstone	x
Y 26	x	lvb*	5.05	874.3	Mudstone	17.13
Y 27	2.02	sa	6.14	863.8	Mudstone	x
Y 28	1.98	lvb	5.3	855.4	Mudstone	15.97
Y 29	x	lvb*	5.71	901.3	Mudstone	x
Y 30	x	lvb*	4.89	895.4	Mudstone	x
Y 31	x	sa*	5	939.45	Siltstone	11.98
Y 32	1.98	lvb	5.26	983.7	Mudstone	x
Y 33	1.96	lvb	5.3	948.3	Siltstone	14.47
Y 34	x	lvb*	4.87	897.8	Mudstone	x
Y 35	1.95	lvb	5.04	940.83	Siltstone	8.86
Y 36	x	lvb*	4.91	943.8	Mudstone	x
Y 37	1.89	lvb	5.37	855.7	Mudstone	11.96
Y 38	1.63	lvb	5.87	506.7	Mudstone	x

Note: x-not analyzed; sa-semianthracites; lvb-low volatile bituminous coal; m vb-medium volatile bituminous coal; *-conjectural results; G_i , total gas content in air dry basis.

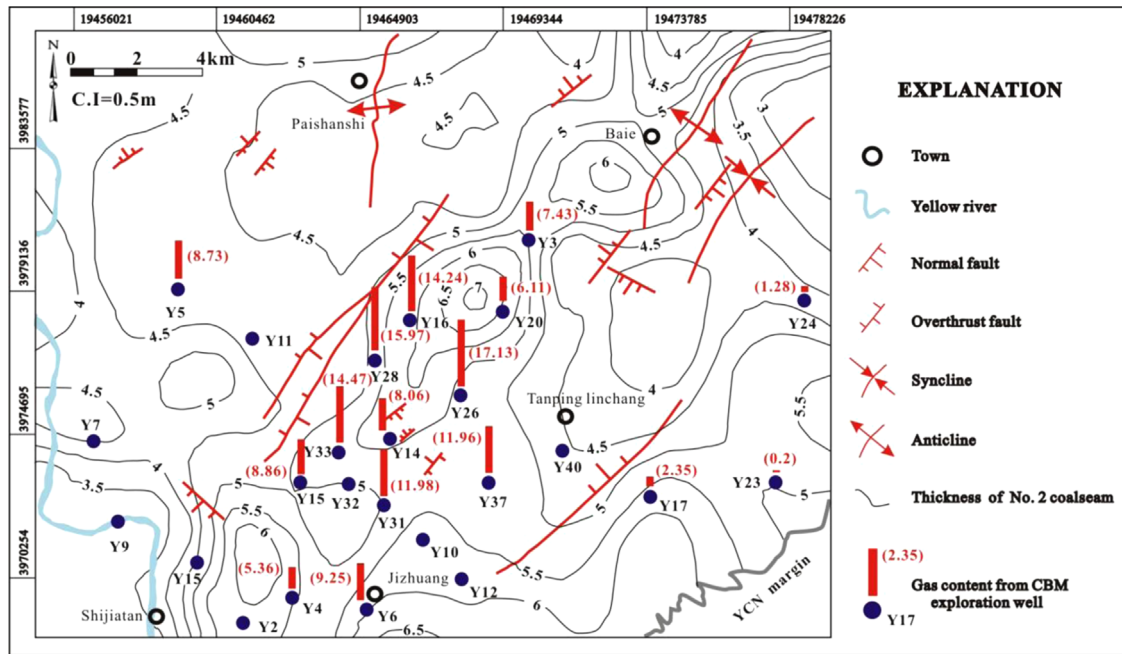


Fig. 5. Gas content and coal thickness of the No. 2 coal seam in the YCN area, SE Ordos Basin.

Table 2
Coal composition and microfractures of coals from the YCN area, southeastern Ordos Basin.

Sample no.	Coal lithotype	Coal mine	Coal macerals (vol%)				$R_{o,m}$ (%)	Microfractures (per 9 cm ²)				Connectivity	Ultimate and proximate analysis (ad%)				
			V	I	L	M		A+B	C	D	Total		Cad	Had	Sad	Mad	Aad
YCN-1	Semi-bright	Donghe	66.9	25.6	5.9	1.6	0.89	1	19	18	39	Poor	76.83	4.55	0.26	1.05	8.44
YCN-2	Dull-semidull		48.4	39.2	9.7	2.7	0.87	2	19	42	64	Poor	80.95	4.35	0.23	1.19	6.22
YCN-3	Dull-semidull		69.4	19.8	10	0.8	0.89	3	17	51	72	Poor	80.87	4.57	0.28	1.06	5.87
YCN-4	Bright	Sangshuping	80.7	15.1	3	1.2	1.56	2	21	27	52	Good	71.22	3.39	2.39	0.25	16.98
YCN-5	Bright		84	11.6	0.6	3.8	1.58	4	24	52	82	Good	71.16	3.59	3.69	0.36	15.55
YCN-6	Bright		46.7	49.1	1.2	3	1.6	0	8	2	12	Poor	63.88	3.21	2.01	0.6	23.41
YCN-7	Bright	Wolonggou	87	9.7	0.4	2.9	1.68	0	13	12	27	Poor	60.29	3.07	0.4	0.53	28.88
YCN-8	Bright		81	14.4	1.1	3.5	1.64	0	14	13	29	Poor	64.44	3.26	0.3	0.38	24.59
YCN-9	Bright		95.6	4.2	0	0.2	1.63	1	11	7	21	Poor	85.67	4	0.33	0.33	5.35

Note: V, vitrinite; I, inertinite; L, liptinite; M, minerals; $R_{o,m}$, Maximum vitrinite reflectance; \odot Microfracture frequency means the numbers of microfractures at the scale of 3×3 cm². Type of microfractures includes Type A, with width (W) ≥ 5 μ m and length (L) ≤ 10 mm; Type B, with $W \geq 5$ μ m and $L \leq 10$ mm; Type C, with $W \leq 5$ μ m and $L \geq 300$ μ m, and Type D, with $W \leq 5$ μ m and $L \leq 300$ μ m. \odot Cad (%), Carbon content (as received basis), Had (%), Hydrogen content (as received basis), Sad (%), Sulfur content (as received basis), Mad(%), Moisture content (as received basis), Aad (%), Ash content (as received basis).

Table 3
Petrophysical results of YCN coals from the southeast Ordos basin, China.

Sample no.	Porosity (%)			Permeability (mD)
	Micro & mesopores	Macropores	Total	
YCN-2	1.24	0.36	1.6	0.016
YCN-3	2.17	0.73	2.9	0.183
YCN-4	1.89	0.51	2.4	1.13
YCN-6	1.83	0.77	2.6	5.52
YCN-7	3.29	0.51	3.8	0.061
YCN-8	1.47	0.33	1.8	0.044

production. Optimum coal rank for CBM production is 1.2–2.5% $R_{o,m}$ (Creedy, 1988; Flores, 1998), because less mature coals ($< 1.2\%$ $R_{o,m}$) generally have lower gas contents and more mature coals ($> 2.5\%$ $R_{o,m}$) have lower permeability. The vitrinite

reflectance of coals pierced by CBM exploration wells are mainly medium volatile bituminous coal (*mvb*) to semi-anthracite with $R_{o,m}$ ranging from 1.48 to 2.2%, with an average of 1.81% (Table 1). Vitrinite reflectance ranges from 0.87% to 1.68% in the samples from the adjacent shallow coal mines of the research area (Table 2). Vitrinite reflectance increases with increased burial depth (Fig. 6) (Pashin, 2010; Cai et al., 2011).

Cooling during the tectonic evolution of the basin should change the shape of the isotherm such that lower temperature coal seams are capable of retaining more gases than higher temperature coals assuming all other coal properties are the same (Scott et al., 1994; Scott, 2002). High gas content areas are usually associated coal that has reached the thermal maturity level required for gas generation. In the early Cretaceous, the basin subsided again, for what became a period of secondary generation of CBM. The YCN area has been exposed to stable deposition and terrestrial heat since its founding on the ancient crystalline basement of the Ordos Basin except for the period of the Yanshanian

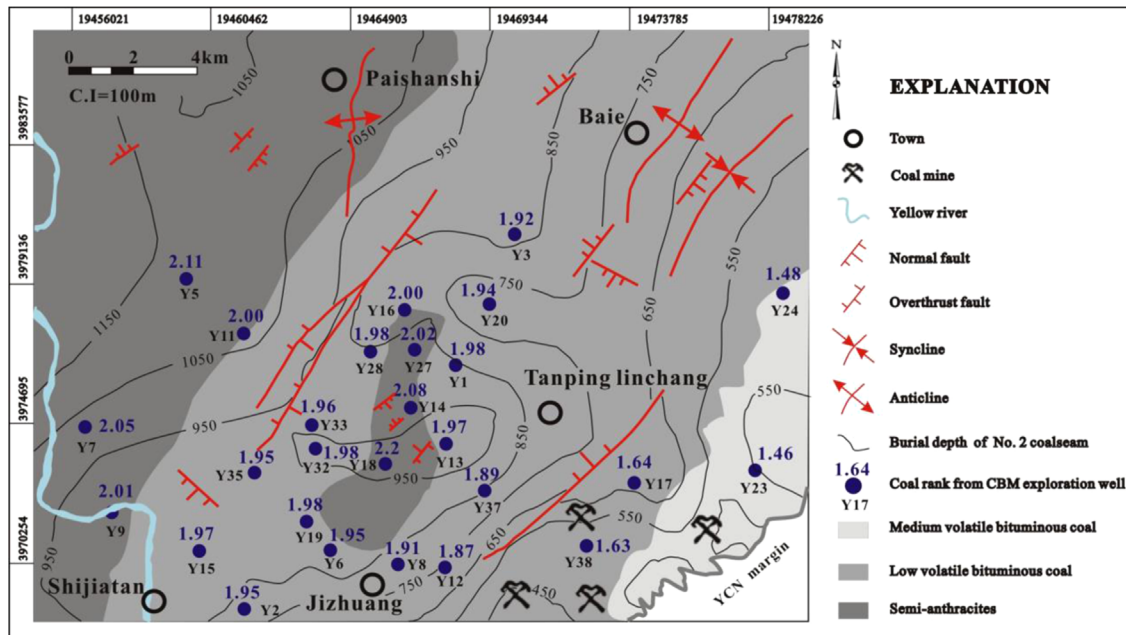


Fig. 6. Overburden depth and vitrinite reflectance ($R_{o,m}$) of the No. 2 coal seam in the YCN area, SE Ordos Basin.

orogenesis. Previous research shows that an abnormally high terrestrial heat flux (from magma intrusion) was present during the Yanshanian orogenesis (Ren et al., 2006; Yang et al., 2006). This abnormally high terrestrial heat flux may have had a slightly positive effect on CBM generation even though the magma intrusion area is 180 km distant from the YCN area and covers merely 23 km². This may have increased the gas content by the secondary generation of thermogenic methane (Fig. 2). Carbon isotope magnitudes range from -29.42% to -38.48% , with an average of -35.47% in methane from the No. 2 coal seam. This indicates that the generated CBM is thermogenic with coalification nearly reaching the rank of anthracite. This implies that the late Yanshanian orogenesis is the main period for gas generation.

4.2. Gas migration

4.2.1. Tectonic evolution

After the middle and late Ordovician the North China platform was overall uplifted due to Caledonian crustal movements. This resulted in unconformity in the sedimentary record from late Ordovician to the early Carboniferous (Yang et al., 2005). Subsidence began again in the middle Carboniferous due to Hercynian crustal movements. The Permo-Carboniferous coal-bearing strata were deposited during this stage. The coal-bearing strata of the Carboniferous and Permian were altered through the Indosinian, Yanshanian and Himalayan orogenies (Fig. 2). Yanshanian and Himalayan tectonic movements had a more important impact on the district via the migration of CBM.

The period of the Carboniferous to the Triassic is the most important stage in the burial history of coal-forming during stable subsidence of the Ordos Basin (Ao et al., 2012). After that, approximately 3000 m of continuous sedimentary strata were deposited in the late Permian-Triassic. The strata experienced a long-term plutonic metamorphism when it was deeply buried. The late Triassic Indosinian orogenesis was relatively strong. At this stage, the Ordos Basin was compressed by the NS trending stress from the collision between the North China and the South China plates. CBM migration occurred during this first adjustment: most of the CBM were sealed in-place due to compressive tectonic loading.

During the Yanshanian orogenesis, the Ordos Basin was compressed again by the NW-SE trending stress from the collision of the Pacific plate and the Eurasian continent. Thus, the eastern edge of the basin developed a series of faults and folds striking to the NE-NNE (Lu et al., 2011). At the same time, the Ordos Basin was compressed in the east by the uplift of the Lvliang Mountains under the NW-SE trending stress. This formed the modern NS trending structure of the formation. In the early stage of the Yanshanian orogenesis, Mesozoic strata were eroded due to large-scale uplift, which reduced overburden on the coal seam. As a result coalification ceased during this stage and gas escaped due to unroofing. Once the coals are saturated with methane during coalification, additional gas generated within the coal will cause overpressure and force lateral migration within the coal seams. Therefore, the presence of laterally continuous coal seams may allow gas from thermally mature areas to migrate updip and to charge lower rank coals. In the YCN area, coals exist in the deep and thermally mature area of the basin, indicating that long and distant lateral migration of CBM from high-rank coals is possible. The relatively low gas content in many shallow coals reflects low coal rank, gas diffusion from the coal, limited secondary biogenic gas generation and/or limited thermogenic and biogenic gas migration.

During the Himalayan orogenesis, due to the collision of the Indian plate and the Eurasian continent with a NE-SW compressive stress, basin tectonics resulted in a negative inversion – this caused the NE-NNE trending fractures or thrust faults to open (Liao et al., 2007). The overlying strata were further eroded, which destroyed CBM equilibrium once again and improved the permeability of coal seams due to the release of overburden stress. Even though some fractures opened and overlying strata eroded in the Himalayan orogenesis, only a few major structures developed in the YCN area (Fig. 2). Overall the structures in the YCN area are simple, the fractures are not developed, and thus the CBM preservation is still relatively favorable.

4.2.2. Hydrodynamics

Hydrodynamics affects gas content through the generation of secondary biogenic gases that increases the gas available for sorption, the development of regional overpressure that may

allows more gases to be adsorbed in the fractures or intergranular pore space. In addition it allows the migration of thermogenic and biogenic gases to impermeable barriers that locally increase gas content, and lowers gas content by water flowing through permeable coal seams (Scott, 2002). Therefore, understanding the hydrodynamics (fluid migration directions and rates) of a system can be very important for predicting the distribution of gas content. The gas content, which is strongly dependent upon hydrodynamic factors, reservoir pressure and temperature (Scott and Kaiser, 1996), will change when the equilibrium conditions of the reservoir are disrupted.

Gas content generally increases where hydrodynamic trapping of CBM occurs (Cai et al., 2011; Karacan et al., 2012; Xu et al., 2012) and may decrease in active recharge areas with downward flow potential or convergent flow where there is no mechanism for entrapment (Scott, 2002). Correlated between wells of the coal and other lithologies has been conducted by the following three steps: (1) constructing the lithology of each well from the well log; (2) constructing 2D seismic sections based on seismic lines; and (3) comparing the lithology from the wells with the lithology interpreted from the seismic section to acquire the coal and other lithology correlated between wells. Based on the generalized section (Fig. 7), hydrodynamic connection of the No. 2 and No. 10 coal seams is precluded by multiple impermeable layers. Groundwater recharge, migration, and discharge are similar in both the No. 2 and No. 10 CBM reservoirs. Therefore, the discussion hereafter will focus on the hydrodynamic features of the No. 2 CBM reservoir.

The roof of the No. 2 coal seam is mudstone in most areas (2–8 m thick). There is a hydrodynamic connection through fractures within the coal seam, which can be regarded as a single aquifer. The groundwater TDS (total dissolved solids) of the No. 2 coal for the SE Ordos Basin ranges from 0.23 g/l to 0.45 g/l, which belongs to the fresh-water plumes (TDS < 10,000 mg/L) (Pashin et al., 2014). Groundwater migration in the aquifer is controlled by tectonics, topography, and precipitation. Precipitation in topographic lows is more easily recharged than in discharge areas. Based on this phenomenon, the ground water flow direction can be acquired. The central two overthrust faults divide the drainage system (Fig. 8). The waters in the central two overthrust faults are low in TDS (0.31–0.34 g/l), which means that fresh water could be connected with the aquifer of No. 2 coal. Importantly, controlled by the extensional stresses of the Himalayanian orogenesis, the central two overthrust faults strike at a high angle to the area margin and are therefore not obstacles to recharge. The extensional large faults appear to conduct large volumes of fluid in the recharge area but may be sealed in the interior of the basin. In the eastern part, the groundwater recharges from the southeastern areas along the margin of the research area, while in the western part, the groundwater recharges from the central two overthrust faults, as well as from the faults toward the deep western part of the YCN area.

In both recharge and discharge areas, groundwater flow reduces CBM content. In deep stagnant areas, however, CBM flows with the groundwater and re-accumulates in the deep zone under water pressure. The gas contents in the area of stagnant ground

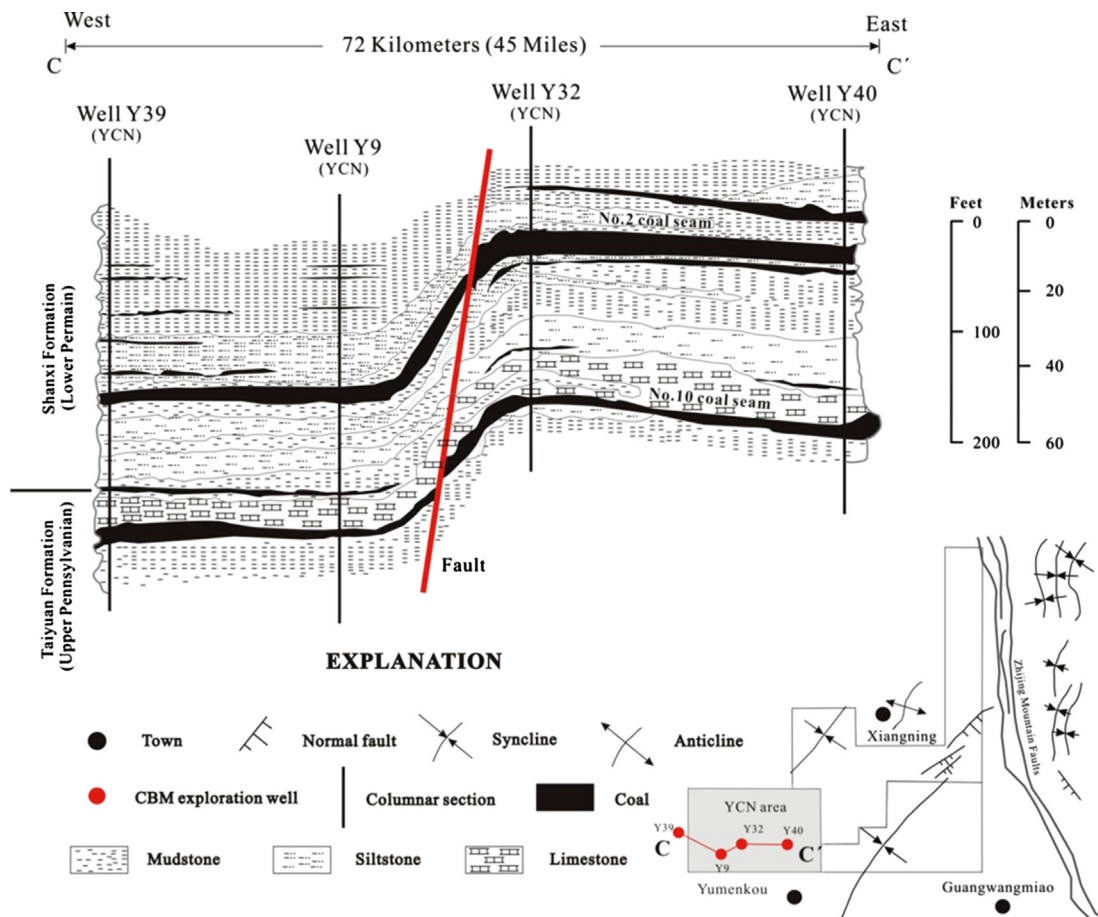


Fig. 7. Generalized cross section C–C' from well Y39 to well Y40 in the YCN area, SE Ordos basin (well location see Fig. 3).

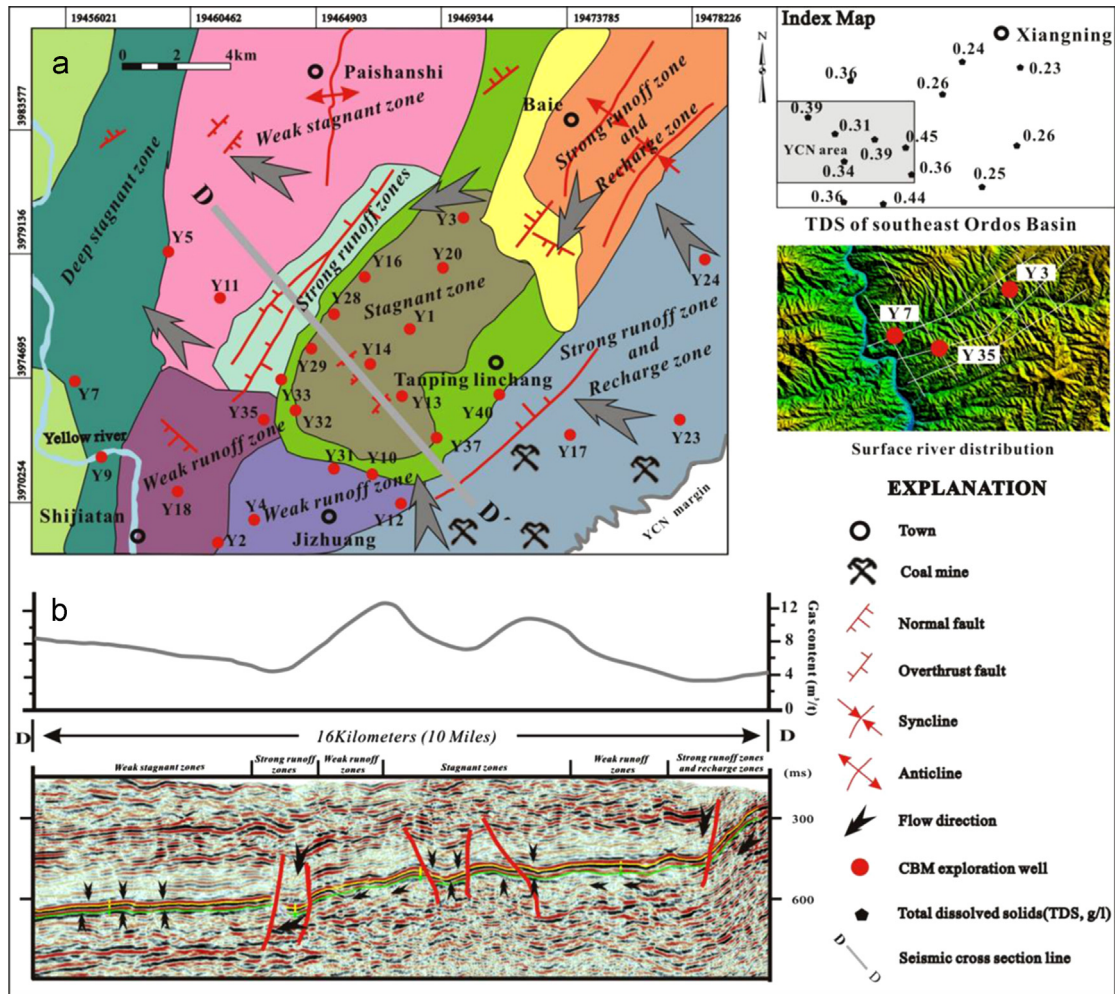


Fig. 8. Gas content and hydrodynamics in the YCN area, SE Ordos Basin. (a) View of flow compartments and flow directions; (b) Cross section of gas content and water flow pathways.

water is higher than that of either the recharge or discharge areas (Fig. 8). Normally the aquifers of the coal-bearing strata have weak-to-moderate water flow, which have relatively strong runoff zones along the faults and the recharge area margin.

4.2.3. Coal thickness and geometry

Where the No. 2 coal seam is thicker than 5 m it normally has high gas contents that are greater than $9 \text{ m}^3/\text{t}$, while seams less than 5 m thick have low gas content. Coal thickness has a strong influence on CBM migration. Although coal thickness is not directly related to gas content, it can affect gas redistribution when tectonic movement or magma intrusion occurs. Thick coal seams may prolong the duration of gas migration, which can cause gas to be distributed heterogeneously. To investigate the preservation of CBM, the overburden depth of the No. 2 coal seam was mapped (Fig. 6). The No. 2 coal overburden depth ranges from 450 to 1200 m and increases toward the northwest. The highest CBM in-place is at overburden depths of 850–1000 m. In the northwest deep zone, the coal thickness decreases to be less than 4 m, which should be an unfavorable factor for CBM preservation.

4.2.4. Reservoir pressure and temperature

The reservoir pressure system was also divided by these two overthrusts (F1 and F2). The measured reservoir pressures are 9.3 MPa–10 MPa in the western and 3.6–4.5 MPa in the eastern compartment. Also apparent is that some gas content also escaped

from the coal seam in the gap between these two compartments. Similarly within these compartments, the hydrostatic pressure gradient is highly variable at 7.6–8.7 KPa/m in the west and 4–4.8 KPa/m in the east and substantially lower than a normal hydrostatic pressure gradient of 9.8 kPa/m. The possible reasons for this low hydrostatic pressure gradient could be the influence of shallow depth, prior mining of coal, geologic structure or hydrodynamics (Pashin, 2010). During the Himalayan orogenesis, the stresses were reversed (Fig. 3). In turn, this opened the previously closed overthrust structures, allowing CBM an easy escape from these structures. This is the reason why the gas contents of coals close to the faults are depleted relative to those away from the faults.

The reservoir temperature is in the range of 31.5–45.4 °C, with an average of 38.4 °C. The temperature gradient for the strata of the YCN ranges from 36.8 °C/km to 37.8 °C/km. Factors including rank, mineral matter, moisture, maceral content, and volatile matter content have long been recognized to correlate strongly with adsorption capacity (Carroll and Pashin, 2003; Pashin et al., 2009). Adsorption isotherm curves are steep at low pressure and flatten at high pressure (Fig. 9) with the shape of the curve exerting a strong impact on reservoir performance. Langmuir pressure, which is the pressure at which gas capacity equals 50% of the Langmuir volume, is an important indicator of the shape of an isotherm. Where reservoir pressure is high and the slope of the isotherm is low, pressure may need to be reduced substantially ($\sim 5 \text{ MPa}$) to desorb a significant proportion of the gas.

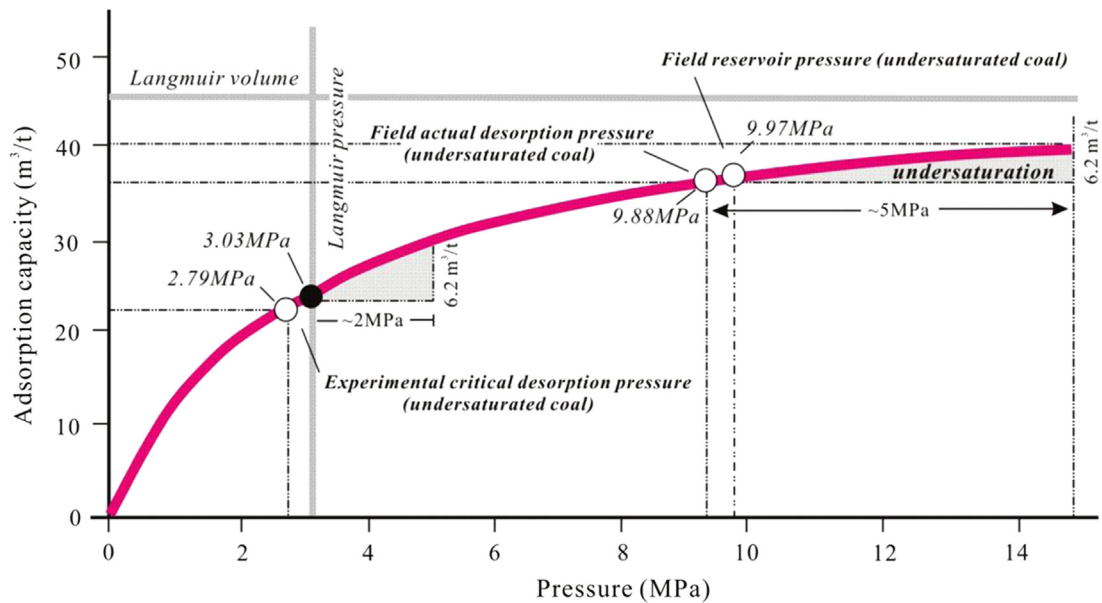


Fig. 9. Absolute adsorption isotherm derived from a coal sample from Well Y7 in the No. 2 coal seam of the YCN area of the SE Ordos Basin showing relationship between Langmuir volume and Langmuir pressure and the impact of undersaturation along different parts of the isotherm curve.

Table 4

Adsorption results of the coals from the No. 2 coal seam in the YCN area.

Well name	P_R (MPa)	V_L (m^3/t)	P_L (MPa)	G_T (m^3/t)	G_S (%)	P_{Tc} (MPa)	P_{RD} (MPa)
Y 1	×	31.86	1.8	×	×	0.82	×
Y 3	3.63	32.2	2.55	18.92	39.27	0.77	2.2
Y 7	9.97	46.51	3.03	35.67	57.14	2.79	9.88
Y 35	4.38	32.18	2.22	21.36	41.48	0.84	3.95
Y 37	3.95	32.36	2.3	20.45	58.48	0.8	3.57

Note: P_R , reservoir pressure; V_L , P_L are Langmuir volume (in air dry basis) and Langmuir pressure; $G_T = V_L P_R / (P_R + P_L)$; $G_S = G_T / G_T$ (G_T from Table 1), gas saturation; P_{Tc} , experimental critical desorption pressure (MPa); P_{RD} , Field real desorption pressure (MPa); x-no analyzed data.

By comparison, where reservoir pressure is low and the slope of the isotherm is high, proportionally smaller changes of reservoir pressure (~ 2 MPa) may only be required to reach the critical desorption pressure, even where the coal is significantly undersaturated (Fig. 9). In the YCN CBM fields, Langmuir pressure averages 2.38 MPa and ranges from 1.8 MPa to 3.03 MPa (Table 4), indicating that the shape of the isotherm curves may vary significantly.

4.3. Gas preservation

4.3.1. Reservoir properties and coal structure

Coal analysis shows that medium volatile bituminous (*mvb*), low volatile bituminous (*lvb*) and semi-anthracites in the YCN are dominated by maceral assemblages of vitrinite and subordinate inertinite and some liptinite. Proximate analysis indicates that the No. 2 coal from the YCN contain 0.25–1.19% moisture, 5.4–28.9% ash yield, 60.3–85.7% carbon and 3.1–4.6% hydrogen (Table 2). The moisture content is low, which should be favorable for CH_4 adsorption. Normally, there is a competitive adsorption between water and CH_4 (Pan et al., 2010). However, because the moisture content varies with coal rank and composition, methane adsorption capacity also changes with these variables. It is difficult to isolate the effects of moisture content (Bustin and Clarkson, 1998).

Minerals in coals have different origin and behavior during coalification, metamorphism and hydrodynamic evolution. Their

presence is mainly controlled by the depositional environments (Vassilev et al., 1997) and tectonic movements. Low volatile matter, sulfur, ash and moisture contents are typically conducive to CBM adsorption. Adsorption isotherms derived at 30 °C indicate that the methane adsorption capacity (i.e., Langmuir volume) of coal in the YCN CBM fields ranges from less than 35 cm^3/g to more than 45 cm^3/g on an air dry basis (Table 4 and Fig. 9). This methane isotherm, measured at 30 °C, would overestimate the real, in-situ, capacities where the real reservoir temperature is between 31.5 °C and 45.4 °C.

CBM reservoirs are often characterized by a pore-fracture (or dual porosity) system including cleats. Porosity of the No. 2 coal from logging data of the exploration wells (Karacan, 2009; Li et al., 2011) is 1.3–4.6%, with an average of 3.3%. This is close to the experimental data of 1.6–3.8% (Table 3). Mercury porosimetry data define the pore size distribution (Table 3). The relationship between adsorption capacity and micropore content shows that a large number of micropores are favorable for gas adsorption in the coal reservoir (Crosdale et al., 1998). Methane is predominantly stored in an adsorbed state in the coal matrix with pores having diameters less than 100 nm. Although the importance of gas migration through the cleat system is well known, diffusion through the coal matrix can also affect gas contents and producibility (Scott, 2002). The process of gas diffusion through the matrix is assumed to be concentration-driven and is modeled using Fick's law of diffusion (Busch et al., 2004; Harpalani and Chen, 1997). Two models representing unipore and bidisperse sorption/diffusion models were used to obtain the diffusion coefficients. The unipore model seems to better represent the sorption kinetics of high rank coals (*mvb* to anthracite) while a bidisperse model better represents low maturity coals (Busch and Gensterblum, 2011). Previous research shows that diffusion rates increase with temperature and decrease with moisture content (Busch et al., 2004; Gruszkiwicz et al., 2009). Methane diffusivity has been measured at 2.93×10^{-7} to 3.70×10^{-5} cm^2/s (Olague and Smith, 1988), while other measured results range from 10^{-8} to 10^{-11} cm^2/s (Clarkson and Bustin, 1999; Cui et al., 2004). Heterogeneity in coal composition (Karacan, 1999), pore structure (Cai et al., 2013) and matrix moisture content (Pan et al., 2010) may vary significantly from coal to coal, which will make the diffusion coefficients variable.

CBM must be first desorbed from the pore surface, then transported by diffusion into the fracture/cleat system and from there to the wellbore by Darcy flow (Ayers, 2002). Therefore the fractures/cleats are the main conduits which contribute to the permeability. The microfracturing frequency of the No. 2 coal is relatively well developed (with an average of 44 per 9 cm^2). However, the microfracture connectivity in the YCN area is not optimal for gas flow. The cleat/fracture porosity (normally lower than 1% for high rank coal) has a positive correlation with permeability (Palmer et al., 2007). From well testing the measured coal reservoir permeability of the YCN area ranges from 0.0124 mD to 0.1735 mD. Based on core plug analysis, there are 5 fractures with fracture spacing ranging from 0.5 cm to 1.4 cm in the coal core recovered from Well Y 35, which has the highest permeability of 0.17 mD. The permeability of the YCN coal is generally lower than 0.2 mD. The deep overburden cover of the No. 2 coal seam and the compressive tectonic stresses most likely contribute to the low permeability in the YCN area. This is favorable for CBM preservation.

The main lithotype is bright coal, which is followed by semi-bright coals. The semi-bright/dull coals (high inertinite, high ash yield) have a greater percentage of mesoporosity and less microporosity than bright or banded bright coals (high vitrinite, low ash) of the same rank (Gan et al., 1972). Based on observations from exploration wells and laboratory experiments (Table 1), most coals from the YCN areas are bright coals. They should therefore be favorable for gas adsorption. Gas is most readily recovered from coals with high macroporosity (Cai et al., 2013). The main lithotype is bright coal for all coal cores, and thus the coal should have high adsorption capability (Fig. 10). While the coal structure differs

significantly from location to location there are no shale stringers within the No. 2 coal seam except in Well Y 3 (Fig. 10) (this is a likely reason for the anomalously low gas content in Well Y 3).

4.3.2. Geologic structure

Data defining gas content come from well testing and includes the measurement of fluxes from lost gases, desorbed gases and residual gases. This gas content was then contoured by map and the Inverse Distance Weighting method used to acquire gas content section lines that were ultimately used to acquire the relationship between geologic structure and gas preservation. In the YCN area, the gas contents are highly variable, ranging from 0.2 to $20.4\text{ m}^3/\text{t}$, which are structurally and hydrodynamically controlled in the order of simple structure (folds and little faults) > complex structure (large regional faults) and groundwater stagnant zones > runoff zones. The gas saturation is 40–100% (generally lower than 70%). In syncline Sc1, gas content is about $4\text{ m}^3/\text{t}$, which is significantly lower than that in the anticline Ac1 ($8\text{ m}^3/\text{t}$) (Fig. 11). This is likely related to the shallow overburden depth of Sc1 that remains unfavorable for the concentration of CBM.

4.3.3. Lithology distribution of roof and floor

Thickness of sediments from the No. 10 coal seam to the No. 2 coal seam ranges from 50 m in the east YCN (well Y40) to 40 m in the west YCN (well Y39). In the east YCN, well Y40 consists of thick mudstone, siltstone, thick limestone, and four coal seams. From the eastern to the western part of the YCN, the number of coal seams increases from five to eight, while the coal thickness is

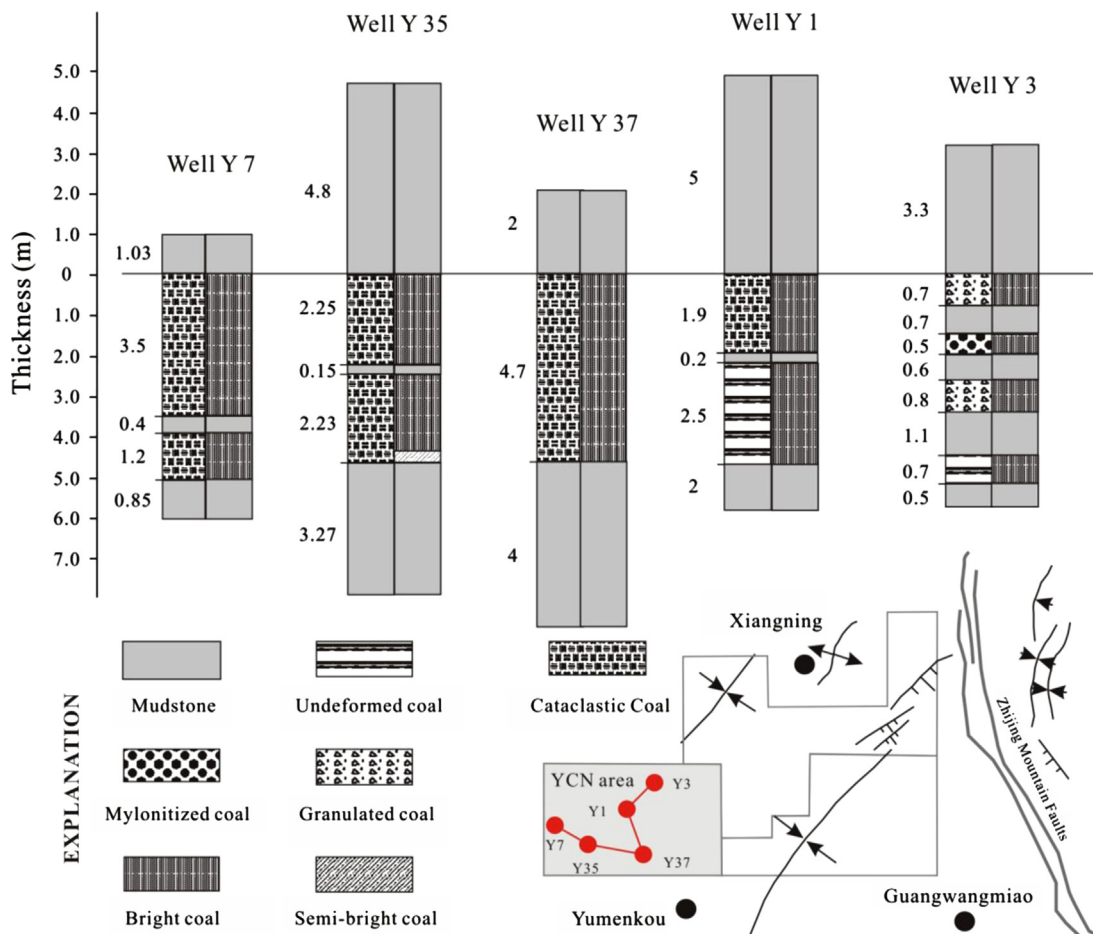


Fig. 10. Coal structure and lithotype of No. 2 coal seam in the YCN area, SE Ordos Basin (for well location see Fig. 3).

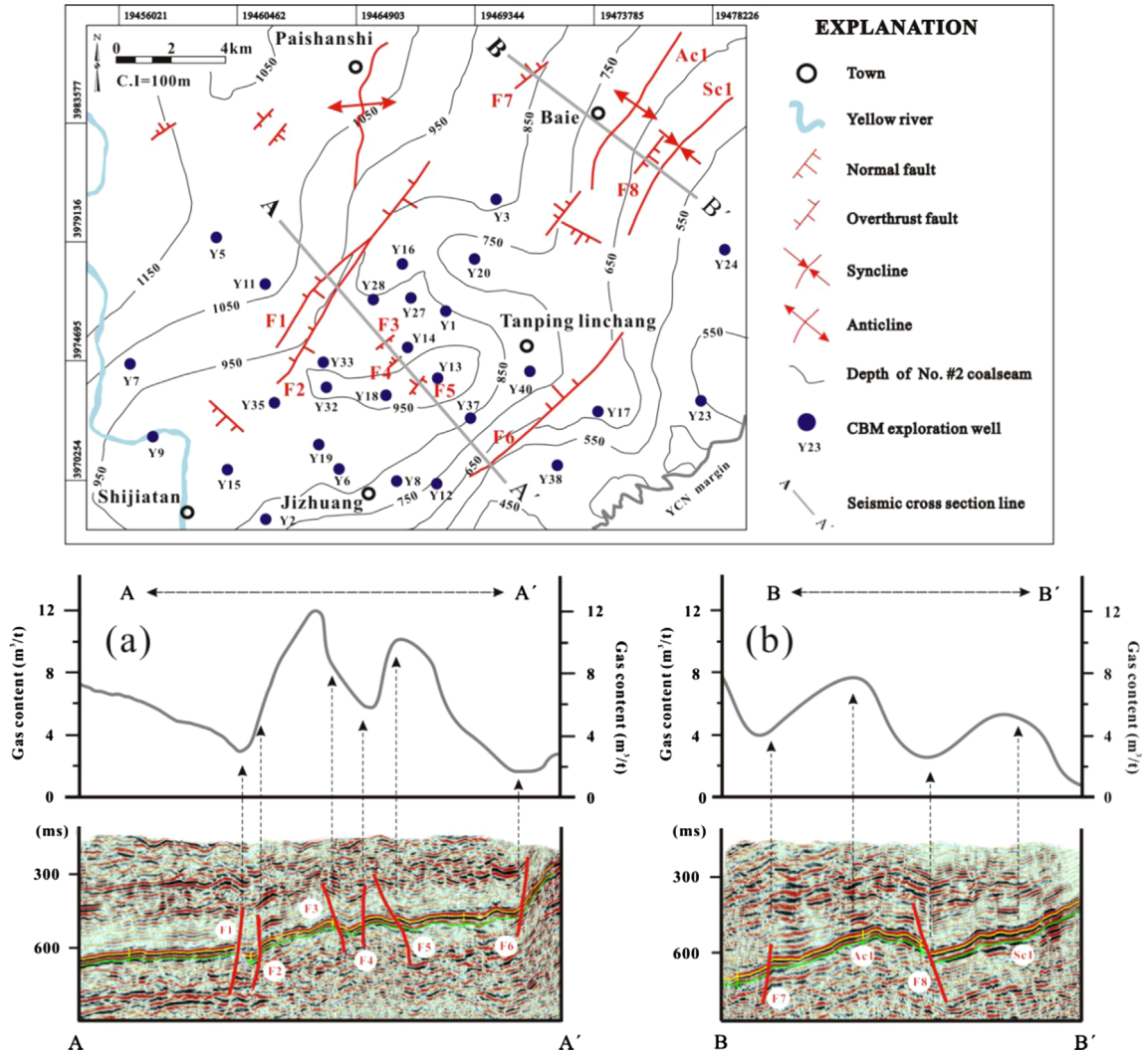


Fig. 11. Comprehensive diagram showing a cross section of structure, gas content and burial depth of the No. 2 coal seam in the YCN area. (a) Cross section A–A' for main faults; (b) Cross section of B–B' main folds.

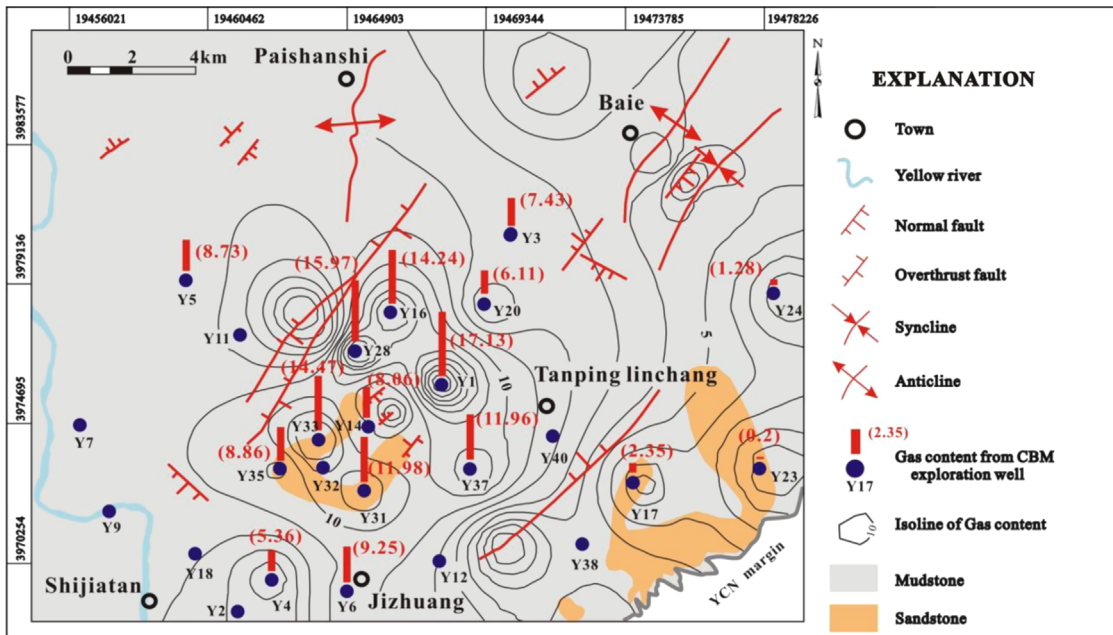


Fig. 12. Isoline diagram of gas content and roof lithology of the No. 2 coal seam in the YCN area, SE Ordos basin.

variable (Fig. 7). The thickness of the No. 2 coal seam decreases from 6 m in the east to 4.5 m in the west. In the western area of the YCN, well Y39 pierces all lithotypes present in well Y40. The roof lithology of the coal seams is mudstone, sandy mudstone and part siltstone. All these lithotypes have good sealing potential and are therefore conducive to CBM storage. But roof lithology of the No. 2 coal seam is mostly mudstone and seals more effectively than siltstone (Fig. 12). Although the seal of the limestone is less tight than that of mudstones and sandstones, fractures are partly sealed by calcite and extensive karst is absent. In all, the limestone roof in the research area provides a partial seal.

The roof and floor lithology and the thickness of the coal seam have a direct influence on CBM preservation. The roof of the No. 2 coal seam is dominated by mudstone and some siltstone (Table 1). The siltstone is distributed mainly in the southeast (wells Y 17 and Y 23) and central south (wells Y 31 and Y 33) areas of the YCN area. The roof thickness of mudstone varies from 0.45 m to nearly 20 m in the YCN area. There is no obvious trend between roof thickness of mudstone and gas content in-place (Fig. 13). This shows that the mudstone normally seals against gas escape even though it is thin, which means that the sealing capability of roof is not only related to its thickness but also its lithology. This could be the reason for a mudstone of about 1 m thick can effectively seal the CBM and retain gas contents of over $10 \text{ m}^3/\text{t}$, such as in Well 31 with a siltstone roof and a gas content of $11.98 \text{ m}^3/\text{t}$. Flow hydrodynamics and the presence of a slight anticlinal trap provides the likely reason for the high gas content of Well 31. Floor properties affecting the gas content are similar to those of the roof (Xu et al., 2012), which can prevent gas dissipation through the base of the coal seam. The floor of the No. 2 coal seam is mainly composed of mudstone and siltstone, which is also favorable for the preservation of CBM.

4.4. Trapping classification of gas content

The CBM concentration (Gas in-place per square kilometer) in the YCN area is estimated as $(0\text{--}1.33) \times 10^8 \text{ m}^3/\text{km}^2$, which is lower than that of the southern Qinshui Basin (Cai et al., 2011). This is recovered using

$$V = H \times D \times C \times 0.01 \quad (1)$$

where V is the CBM concentration (GIP per square kilometer, $\times 10^8 \text{ m}^3/\text{km}^2$) and 0.01 is the adjustment coefficient for the GIP unit. H is net accumulative coal thickness (m); D represents coal density (here set to $1.45 \text{ g}/\text{cm}^3$ based on measurements); C is the gas content from field measurements (m^3/t). Gas concentration decreases from the central coal district (between faults F2 and F6) to the boundary of the research area. It is generally greater than $0.5 \times 10^8 \text{ m}^3/\text{km}^2$ in the central area, which should be favorable for CBM development.

Based on the different gas trapping mechanisms, the CBM concentration is classified into three blocks, block A and C with low gas concentration and block B with high gas concentration (Fig. 14). The main mechanism for gas trapping in block A is roof lithology. Although the coal seams have moderate burial depth and favorable roof lithology, the thickness of the coals is unfavorable for gas migration. Without sufficient source of gas both from this seam and from below, it has not accumulated an adequate supply. For block B, the main mechanism for gas trapping is suitable hydrodynamics and an adequate structural setting. Hydrodynamic trapping is also an important mechanism for increasing gas contents. Water flows are often associated with the landward pinch-out of coal seams, offset of coal seams by faults, and/or areas of high cleat density. At the center of block B, a shallow anticlinal structure makes hydrodynamic trapping possible thus leaving this as a prospective target for CBM development. For

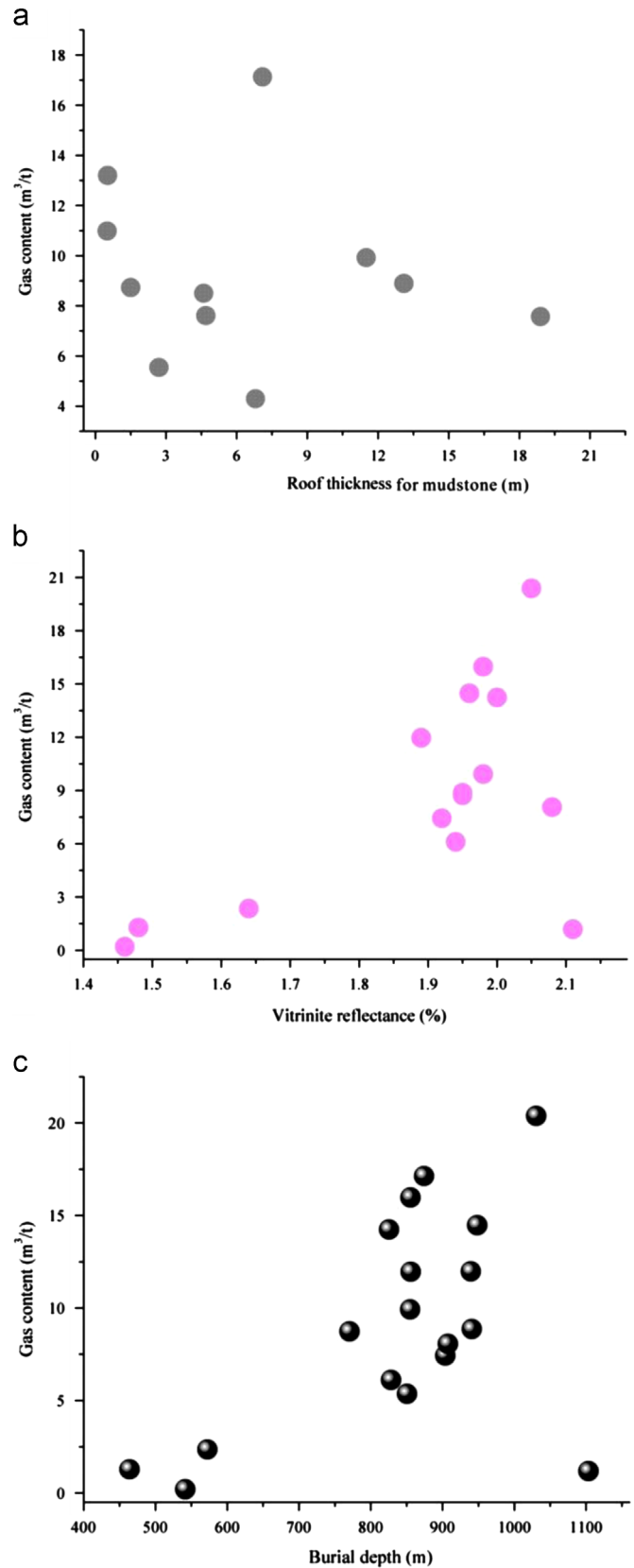


Fig. 13. Relationship of roof thickness of mudstone, vitrinite reflectance, burial depth and gas content of the No. 2 coal seam in the YCN area, SE Ordos basin.

block C, the main mechanism for gas trapping is the presence of a thick coal seam and a low-permeability roof. Although both of these conditions exist, flushing of gases by both meteoric water and

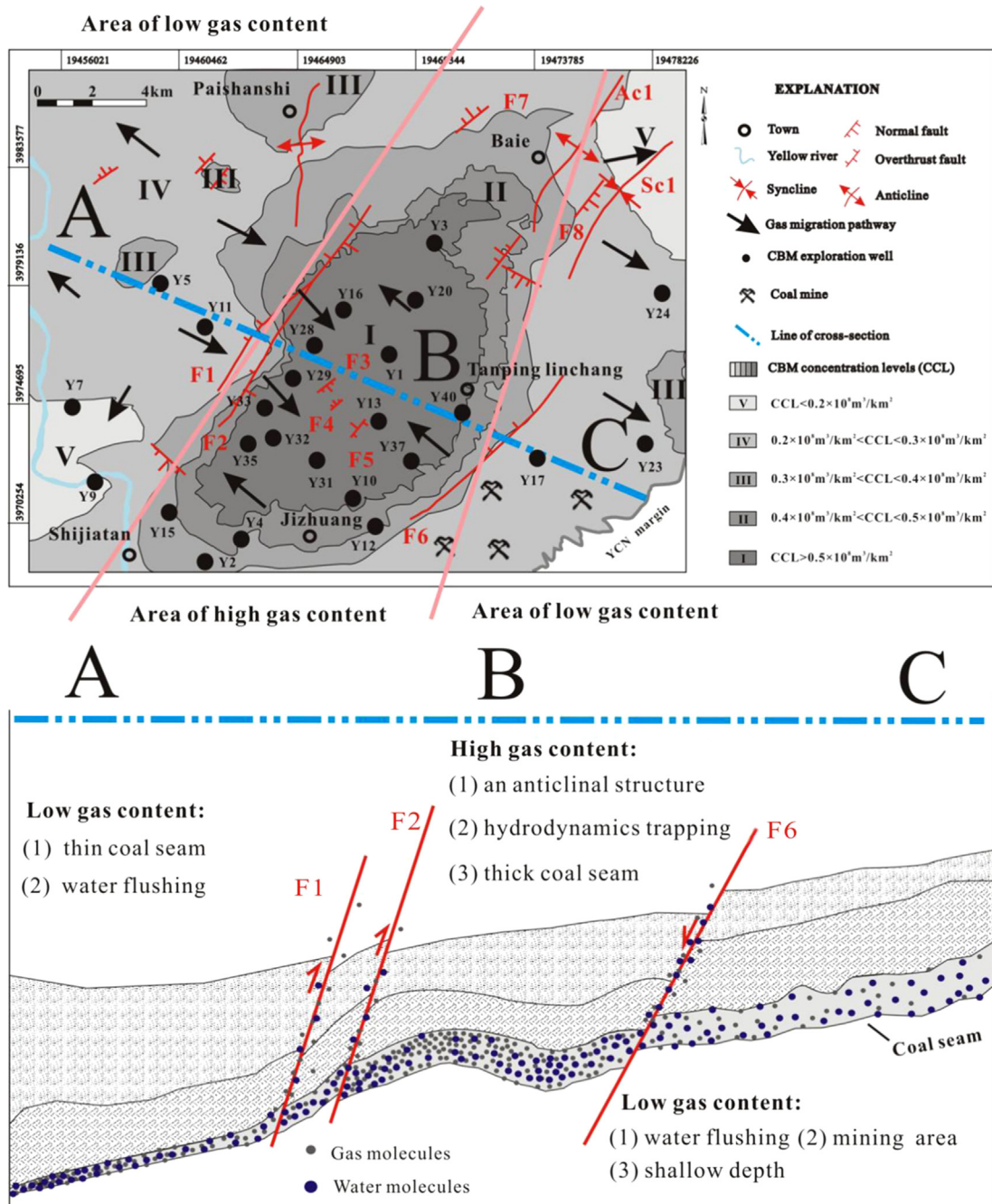


Fig. 14. Evaluation subareas for CBM concentration potential and trapping classification of the No. 2 coal seam in the YCN area, SE Ordos Basin.

groundwater near the recharge zone has resulted in low gas concentrations. Another reason for the low relative gas content may be the presence of many coal mines that were once active in this block.

5. Conclusions

The No. 2 coal seam in the YCN area has a significant potential for CBM exploration and production. Coal rank across the YCN area ranges from medium-volatile bituminous to semi-anthracite. Gas contents vary by two orders of magnitude and are in the range of 0.2–20.4 m³/t in the No. 2 coal seam. This large variability in gas

content results from many geological factors and reservoir characteristics. These include:

1. Gas contents in coal seams are not fixed in time nor space but change when equilibrium conditions in the reservoir are disrupted. Gas content distribution in these coal seams is affected by many geologic factors and reservoir characteristics that may be classified into three principal categories: gas generation, gas migration, and gas preservation.
2. Highly variable gas contents in coals of the YCN area reflect a dynamic history in which tectonics, reservoir pressure, and basin hydrodynamics have been transient over geologic time. During the late stage of the influencing orogenies, fresh-water recharge along the overthrusts F1 and F2 and the southeastern

margin of the YCN area began influencing basin hydrodynamics. These faults compartmentalized the CBM reservoir into two isolated components and set the stage for late-stage methanogenesis.

- Variability of coal thickness and structure affects the distribution of gas content both locally and regionally. Differences in coal properties (including macerals, minerals and moisture content), coal structure and coal petrophysical conditions (including pore structure and the fracture/cleat system) result in significant differences in gas content both locally within individual seams and vertically within thicker coal seams.
- In the YCN, the most favorable area for CBM exploration and development is in block B, which has multiple favorable features aiding CBM generation, migration, accumulation and retention. These include significant coal thickness, moderate burial depth, favorable hydrodynamics and the presence of a shallow anticlinal structure. Such favorable areas for CBM exploration and development appear a composite result of gas generation, gas migration and gas preservation.

Acknowledgments

This project was financially supported by the National Major Research Program for Science and Technology of China (2011ZX05034-001, 2011ZX05062-006), the United Foundation from the National Natural Science Foundation of China, the Petrochemical Foundation of PetroChina (U1262104), the Program for New Century Excellent Talents in University (NCET-11-0721), the Foundation for the Author of National Excellent Doctoral Dissertation of PR China (201253), and the Fundamental Research Funds for the Central Universities (Grant no. 2652013006). In addition, the authors gratefully acknowledge the China Scholarship Council for the joint PHD program and Sinopec for supplying literature information, basic data and production data of CBM wells in the YCN area.

References

- Ao, W., Huang, W., Weng, C., Xiao, X., Liu, D., Tang, X., Chen, P., Zhao, Z., Wan, H., Finkelman, R.B., 2012. Coal petrology and genesis of Jurassic coal in the Ordos Basin, China. *Geosci. Front.* 3, 85–95.
- Ayers Jr., W.B., 2002. Coalbed gas systems, resources, and production and a review of contrasting cases from the San Juan and Powder River basins. *AAPG Bull.* 86 (11), 1853–1890.
- Busch, A., Gensterblum, Y., 2011. CBM and CO₂-ECBM related sorption processes in coal: a review. *Int. J. Coal Geol.* 87, 49–71.
- Busch, A., Gensterblum, Y., Krooss, B.M., Littke, R., 2004. Methane and carbon dioxide adsorption-diffusion experiments on coal: upscaling and modeling. *Int. J. Coal Geol.* 60, 151–168.
- Bustin, R.M., Clarkson, C.R., 1998. Geological controls on coalbed methane reservoir capacity and gas content. *Int. J. Coal Geol.* 38, 3–26.
- Cai, Y., Liu, D., Pan, Z., Yao, Y., Li, J., Qiu, Y., 2013. Pore structure and its impact on CH₄ adsorption capacity and flow capability of bituminous and subbituminous coals from Northeast China. *Fuel* 103, 258–268.
- Cai, Y., Liu, D., Yao, Y., Li, J., Qiu, Y., 2011. Geological controls on prediction of coalbed methane of No.3 coal seam in Southern Qinshui Basin, North China. *Int. J. Coal Geol.* 88, 101–112.
- Carroll, R.E., Pashin, J.C., 2003. Relationship of sorption capacity to coal quality: CO₂ sequestration potential of coalbed methane reservoirs in the Black Warrior Basin. In: *Proceedings of the International Coalbed Methane Symposium*. University of Alabama, Tuscaloosa, Paper 0317. 11 pp.
- Clarkson, C.R., Bustin, R.M., 1999. The effect of pore structure and gas pressure upon the transport properties of coal: a laboratory and modeling study. 1. Isotherms and pore volume distributions. *Fuel* 78, 1333–1344.
- Connell, L.D., Sander, R., Pan, Z., Camilleri, M., Heryanto, D., 2011. History matching of enhanced coal bed methane laboratory core flood tests. *Int. J. Coal Geol.* 87, 128–138.
- Creedy, D.P., 1988. Geological controls on the formation and distribution of gas in British coal measure strata. *Int. J. Coal Geol.* 10, 1–31.
- Crosdale, P.J., Beamish, B.B., Valix, M., 1998. Coalbed methane sorption related to coal composition. *Int. J. Coal Geol.* 35, 147–158.
- Cui, X., Bustin, R.M., Dipple, G., 2004. Selective transport of CO₂, CH₄, and N₂ in coals: insights from modeling of experimental gas adsorption data. *Fuel* 83, 293–303.
- Fallgren, P.H., Zeng, C., Ren, Z., Lu, A., Ren, S., Jin, S., 2013. Feasibility of microbial production of new natural gas from non-gas-producing lignite. *Int. J. Coal Geol.* 115, 79–84.
- Feng, S., Ye, J., Zhang, S., 2002. Coalbed methane resources in the Ordos Basin and its development potential. *Geol. Bull. China* 21 (10), 658–662 (in Chinese with an English abstract).
- Flores, R.M., 1998. Coalbed methane: from hazard to resource. *Int. J. Coal Geol.* 35, 3–26.
- Gan, H., Nandi, S.P., Walker, P.L., 1972. Nature of the porosity in American coals. *Fuel* 51, 272–277.
- Gensterblum, Y., Merkel, A., Busch, A., Krooss, B.M., Littke, R., 2014. Gas saturation and CO₂ enhancement potential of coalbed methane reservoirs as a function of depth. *AAPG Bull.* 98 (2), 395–420.
- Gruszkiewicz, M.S., Naney, M.T., Blencoe, J.G., Cole, D.R., Pashin, J.C., Carroll, R.E., 2009. Adsorption kinetics of CO₂, CH₄, and their equimolar mixture on coal from the Black Warrior Basin, West-Central Alabama. *Int. J. Coal Geol.* 77, 23–33.
- Harpalani, S., Chen, G., 1997. Influence of gas production induced volumetric strain on permeability of coal. *Geotech. Geol. Eng.* 15, 303–325.
- Jie, M., 2010. Prospects in coalbed methane gas exploration and production in the eastern Ordos Basin. *Nat. Gas Ind.* 30 (6), 1–6 (in Chinese with an English abstract).
- Karacan, C.Ö., 1999. Heterogeneity effects on the gas storage and production of gas from coal seams. SPE Paper 56551. In: *Society of Petroleum Engineers 1999 Annual Technical Conference and Exhibition*, Houston, Texas, October 3–9, pp. 479–493.
- Karacan, C.Ö., 2009. Reservoir rock properties of coal measure strata of the Lower Monongahela Group, Greene County (Southwestern Pennsylvania), from methane control and production perspectives. *Int. J. Coal Geol.* 78, 47–64.
- Karacan, C.Ö., Olea, R.A., Goodman, G., 2012. Geostatistical modeling of the gas emission zone and its in-place gas content for Pittsburgh-seam mines using sequential Gaussian simulation. *Int. J. Coal Geol.* 90–91, 50–71.
- Karacan, C.Ö., Ruiz, F.A., Cote, M., Phipps, S., 2011. Coal mine methane: a review of capture and utilization practices with benefits to mining safety and to greenhouse gas reduction. *Int. J. Coal Geol.* 86, 121–156.
- Li, J., Liu, D., Yao, Y., Cai, Y., Qiu, Y., 2011. Evaluation of the reservoir permeability of anthracite coals by geophysical logging data. *Int. J. Coal Geol.* 87, 121–127.
- Liao, C., Zhang, Y., Wen, C., 2007. Structural styles of the eastern boundary zone of the Ordos Basin and its regional tectonic significance. *Acta Geol. Sin.* 81 (4), 466–474.
- Liu, H., Sang, S., Wang, G., Li, M., Xu, H., Liu, S., Li, J., Ren, B., Zhao, Z., Xie, Y., 2014. Block scale investigation on gas content of coalbed methane reservoirs in Southern Qinshui Basin with statistical model and visual map. *J. Pet. Sci. Eng.* 114, 1–14.
- Lu, Y., Zhang, F., Wu, Y., Ji, L., Liu, C., Tian, L., Liu, C., 2011. Analysis of potentials of CBM resources in Yanchuannan Region. *China Coalbed Methane* 8 (4), 13–17 (in Chinese with an English abstract).
- Olague, N.E., Smith, D.M., 1988. Diffusion of gases in American coals. *Fuel* 68, 1381–1387.
- Palmer, I.D., Mavor, M., Gunter, B., 2007. Permeability changes in coal seams during production and injection. In: *Proceedings of the International Coalbed Methane Symposium*. University of Alabama, Tuscaloosa, Paper 0713.
- Pan, Z., Connell, L.D., Camilleri, M., Connelly, L., 2010. Effects of matrix moisture on gas diffusion and flow in coal. *Fuel* 89, 3207–3217.
- Pashin, J.C., 2010. Variable gas saturation in coalbed methane reservoirs of the Black Warrior Basin: Implications for exploration and production. *Int. J. Coal Geol.* 82, 135–146.
- Pashin, J.C., McIntyre, M.R., Carroll, R.E., Groshong Jr., R.H., Bustin, R.M., 2009. Carbon sequestration and enhanced recovery potential of mature coalbed methane reservoirs in the Black Warrior Basin. *AAPG Stud. Geol.* 59, 125–147.
- Pashin, J.C., McIntyre, M.R., Mann, S.D., Kopaska-Merkel, D.C., Varonka, M., Orem, W., 2014. Relationships between water and gas chemistry in mature coalbed methane reservoirs of the Black Warrior Basin. *Int. J. Coal Geol.* 126, 92–105.
- Ren, Z.L., Zhang, S., Gao, S.L., Cui, J.P., Liu, X.S., 2006. Research on region of maturation anomaly and formation time in Ordos Basin. *Acta Geol. Sin.* 80, 674–684.
- Scott, A.R., 2002. Hydrogeologic factors affecting gas content distribution in coal beds. *Int. J. Coal Geol.* 50, 363–387.
- Scott, A.R., Kaiser, W.R., 1996. Factors affecting gas-content distribution in coal beds: a review (exp. abs.). Expanded abstracts volume. *Rocky Mountain Section Meeting: AAPG*, 101–106.
- Scott, A.R., Kaiser, W.R., Ayers Jr., W.B., 1994. Thermogenic and secondary biogenic gases, San Juan Basin, Colorado and New Mexico—implications for coalbed gas producibility. *AAPG Bull.* 78 (8), 1186–1209.
- Song, Y., Liu, H., Hong, F., Qin, S., Liu, S., Li, G., Zhao, M., 2012. Syncline reservoir pooling as a general model for coalbed methane (CBM) accumulations: mechanisms and case studies. *J. Pet. Sci. Eng.* 88–89, 5–12.
- Su, X., Lin, X., Liu, S., Zhao, M., Song, Y., 2005. Geology of coalbed methane reservoirs in the southeast Qinshui Basin of China. *Int. J. Coal Geol.* 62, 197–210.
- Stauffer, P.H., Surdam, R.C., Jiao, Z., Miller, T.A., 2009. Combining geologic data and numerical modeling to improve estimates of the CO₂ sequestration potential of the Rock Springs Uplift, Wyoming. *Energy Proc.* 1 (1), 2717–2724.
- Tang, X., Zhang, J., Shan, Y., Xiong, J., 2012. Upper Paleozoic coal measures and unconventional natural gas system of the Ordos Basin. *China Geosci. Front.* 3, 863–873.

- Tao, S., Wang, Y., Tang, D., Xu, H., Lv, Y., He, W., Li, Y., 2012. Dynamic variation effects of coal permeability during the coalbed methane development process in the Qinshui Basin, China. *Int. J. Coal Geol.* 93, 16–22.
- Vassilev, S.V., Kitano, K., Vassileva, C.G., 1997. Relations between ash yield and chemical and mineral composition of coals. *Fuel* 76, 3–8.
- Wei, C., Qin, Y., Wang, G., Fu, X., Zhang, Z., 2010. Numerical simulation of coalbed methane generation, dissipation and retention in SE edge of Ordos Basin, China. *Int. J. Coal Geol.* 82, 147–159.
- Xu, H., Tang, D., Liu, D., Tang, S., Yang, F., Chen, X., He, W., Deng, C., 2012. Study on coalbed methane accumulation characteristics and favorable areas in the Binchang area, southwestern Ordos Basin, China. *Int. J. Coal Geol.* 95, 1–11.
- Yang, X.K., Yang, Y.H., Ji, L.D., Su, C.Q., Zheng, M.L., Zhao, L., 2006. Stages and characteristics of thermal actions in eastern part of Ordos Basin. *Acta Geol. Sin.* 80, 705–711.
- Yang, Y., Li, W., Ma, L., 2005. Tectonic and stratigraphic controls of hydrocarbon systems in the Ordos Basin: a multicycle cratonic basin in the central China. *AAPG Bull.* 89 (2), 255–269.
- Yao, Y., Liu, D., Qiu, Y., 2013. Variable gas content, saturation, and accumulation characteristics of Weibei coalbed methane pilot-production field in the south-eastern Ordos Basin, China. *AAPG Bull.* 97 (8), 1371–1393.
- Yao, Y., Liu, D., Tang, D., Tang, S., Che, Y., Huang, W., 2009. Preliminary evaluation of the coalbed methane production potential and its geological controls in the Weibei Coalfield, southeastern Ordos Basin, China. *Int. J. Coal Geol.* 78, 1–15.
- Zhang, S., Tang, S., Tang, D., Pan, Z., Yang, F., 2010. The characteristics of coal reservoir pores and coal facies in Liulin district, Hedong coal field of China. *Int. J. Coal Geol.* 81, 117–127.
- Zhang, K., Cai, Y., He, Z., Zhang, B., 2011. Analysis on geological control characteristics of coalbed methane at Yanchuannan block southern Ordos Basin. *Coal Tech* 30 (4), 129–131 (In Chinese with an English abstract).